JBC RESEARCH ARTICLE

Structural basis of T cell receptor specificity and cross-reactivity of two HLA-DQ2.5-restricted gluten epitopes in celiac disease

Received for publication, October 15, 2021, and in revised form, January 15, 2022 Published, Papers in Press, January 21, 2022,
https://doi.org/10.1016/j.jbc.2022.101619

Laura Ciacchi[1], Carine Farenc[1], Shiva Dahal-Koirala[2,3], Jan Petersen[1], Ludvig M. Sollid[2,3], Hugh H. Reid[1], and Jamie Rossjohn[1,4,*]

From the [1]Infection and Immunity Program and Department of Biochemistry and Molecular Biology, Biomedicine Discovery Institute, Monash University, Clayton, Victoria, Australia; [2]Department of Immunology, University of Oslo and Oslo University Hospital-Rikshospitalet, Oslo, Norway; [3]K. G. Jebsen Centre for Coeliac Disease Research, Institute of Clinical Medicine, University of Oslo, Oslo, Norway; [4]Institute of Infection and Immunity, School of Medicine, Cardiff University, Cardiff, United Kingdom

Edited by Peter Cresswell

Celiac disease is a T cell-mediated chronic inflammatory condition often characterized by human leukocyte antigen (HLA)-DQ2.5 molecules presenting gluten epitopes derived from wheat, barley, and rye. Although some T cells exhibit cross-reactivity toward distinct gluten epitopes, the structural basis underpinning such cross-reactivity is unclear. Here, we investigated the T-cell receptor specificity and cross-reactivity of two immunodominant wheat gluten epitopes, DQ2.5-glia-α1a (PFPQPELPY) and DQ2.5-glia-ω1 (PFPQPEQPF). We show by surface plasmon resonance that a T-cell receptor alpha variable (TRAV) 4$^+$-T-cell receptor beta variable (TRBV) 29-1$^+$ TCR bound to HLA-DQ2.5-glia-α1a and HLA-DQ2.5-glia-ω1 with similar affinity, whereas a TRAV4$^-$ (TRAV9-2$^+$) TCR recognized HLA-DQ2.5-glia-ω1 only. We further determined the crystal structures of the TRAV4$^+$-TRBV29-1$^+$ TCR bound to HLA-DQ2.5-glia-α1a and HLA-DQ2.5-glia-ω1, as well as the structure of an epitope-specific TRAV9-2$^+$-TRBV7-3$^+$ TCR-HLA-DQ2.5-glia-ω1 complex. We found that position 7 (p7) of the DQ2.5-glia-α1a and DQ2.5-glia-ω1 epitopes made very limited contacts with the TRAV4$^+$ TCR, thereby explaining the TCR cross-reactivity across these two epitopes. In contrast, within the TRAV9-2$^+$ TCR-HLA-DQ2.5-glia-ω1 ternary complex, the p7-Gln was situated in an electrostatic pocket formed by the hypervariable CDR3β loop of the TCR and Arg70β from HLA-DQ2.5, a polar network which would not be supported by the p7-Leu residue of DQ2.5-glia-α1a. In conclusion, we provide additional insights into the molecular determinants of TCR specificity and cross-reactivity to two closely-related epitopes in celiac disease.

Celiac disease (CeD) is a chronic inflammatory disorder of the small intestine triggered by ingestion of dietary gluten that affects ~1% of the general population (1, 2). Celiac disease is restricted to genetically predisposed individuals, with 95% of patients expressing human leukocyte antigen (HLA) HLA-DQ2.5 (encoded by *DQA1*05:01-DQB1*02:01* alleles) and the remainder HLA-DQ8 (encoded by *DQA1*03:01-DQB1*03:02* alleles) or HLA-DQ2.2 (encoded by *DQA1*02:01 -DQB1*02:02* alleles) (1, 2). Celiac disease pathogenesis is characterized by gluten presentation by the HLA-DQ2.5/8/2.2 molecules on the surface of antigen-presenting cells and recognition by CD4$^+$ αβ T cells (3–12). The gluten peptides that stimulate T cell reactivity, derived from wheat (gliadin), barley (hordein), and rye (secalin) are modified by the transglutaminase 2 (TG2) enzyme (13–16). Transglutaminase 2 is a ubiquitously expressed enzyme that catalyzes the deamidation of gluten peptides by converting glutamine residues to glutamate, thereby conferring upon these peptides the preferred acidic residues for either the P4 or P6 anchor pockets of HLA-DQ2.5/2.2 and P1 and P9 anchor pockets for HLA-DQ8 (17–21). These TG2-deamidated gluten peptides bind with increased affinity to the HLA, thereby stabilizing the complex thus allowing for sustained antigen presentation by APCs and, subsequently, more frequent recognition by gluten-specific CD4$^+$ T cells (5). The CD4$^+$ T cells then provide help to B cells that bind TG2-gliadin complexes and deamidated gluten peptides to mature into plasma cells in the gut that generate deamidated gluten peptide-specific, as well as autoreactive TG2-specific, antibodies (8, 22, 23).

In HLA-DQ2.5$^+$ CeD, the main immunodominant gluten epitopes that elicit strong T cell responses include (using the nomenclature system developed by Sollid *et al.* (2020)) DQ2.5-glia-α1a/α2 (PFPQPELPY/PQPELPYPQ), DQ2.5-glia-ω1/ω2 (PFPQPEQPF/PQPEQPFPW), DQ2.5-hor-1/sec-1 (PFPQPEQPF), and DQ2.5-hor-3 (PIPEQPQPY) (10, 11, 18, 19, 24–30). The responding CD4$^+$ αβ T cell repertoire toward these epitopes in HLA-DQ2.5$^+$ CeD patients are characterized by biased *TRAV/TRBV* gene expression of T cell receptor (TCRs) (4, 18, 19, 21, 27).

Owing to the high sequence similarity between DQ2.5-glia-α1a and DQ2.5-glia-ω1 epitopes, the TCR repertoires have shared features such as the predominance of expanded T cell clones (TCCs) with *TRAV4*, *TRBV20-1*, or *TRBV29-1* gene usage (18, 19). In addition, frequent usage of these genes was observed in the DQ2.5-glia-α2/ω2 and DQ2.5-hor-3 responses (4, 18, 19, 24, 27). Apart from these genes, there was also frequent *TRAV9-1/2* and

* For correspondence: Jamie Rossjohn, Jamie.rossjohn@monash.edu.

TRBV7-2/3 gene usage among the DQ2.5-glia-α1a/α2- and DQ2.5-glia-ω1/ω2-reactive TCCs (18, 26, 27). The biased gene usage of CeD TCRs observed across multiple epitopes presented by the same HLA-DQ2.5 is indicative that these TCRs have a dependence on interactions with this HLA.

Structural studies have provided insights into how TCRs recognize immunodominant HLA-DQ2.5-gliadin complexes. To date, these structures have examined TCRs that are binding to one HLA-DQ2.5-gliadin complex, with this process henceforth referred to as specific TCR recognition to delineate from cross-reactive TCR recognition, whereby TCRs are binding to more than one HLA-DQ2.5-gliadin. The three ternary structures of TRAV26-1$^+$-TRBV7-2$^+$ TCRs specific for DQ2.5-glia-α2 revealed that a conserved CDR3β-Arg residue formed essential contacts with p5-Leu and position 7 (p7)-Tyr within DQ2.5-glia-α2 epitope (19). The ternary structure of a TRAV4$^+$-TRBV20-1$^+$ TCR specific for DQ2.5-glia-α1a did not contain a conserved Arg residue and recognition was mainly attributed to CDR3 loop-mediated interactions at the interface. This indicated a differing mode of recognition to DQ2.5-glia-α2, as the central region of the DQ2.5-glia-α1a peptide was not contacted by the TCR. However, there were also similarities in epitope-specific recognition of DQ2.5-glia-α1a and DQ2.5-glia-α2 such as the HLA-interactions mediated by conserved germline-encoded residues between the related TRAV4 and TRAV26-1 α-chains (19). In further studies, we showed that TCRs specific for either DQ2.5-glia-α1a/α2 can cross-react with bacterial mimics of these gliadin epitopes (9). This provided structural evidence to suggest that molecular mimicry may drive cross-reactivity in CeD as the TCR focuses recognition on a few key peptide residues, as suggested previously in some T cell-mediated autoimmune diseases (9, 31–33). Other studies have identified small populations of cross-reactive DQ2.5-glia-α1a/ω1 TCCs and cross-reactive DQ2.5-glia-α2/ω2 TCCs in CeD patients (18, 19, 27). Of note, *TRAV4* gene usage was observed in TCCs specific for DQ2.5-glia-α1a and DQ2.5-glia-ω1, as well as those that were cross-reactive for these epitopes. In addition, studies have shown that grain toxicity of barley and rye may result from cross-reactive T cell responses toward wheat ω-gliadin and homologous hordein- and secalin-derived peptides (4, 15, 24, 30, 34). However, the disease-relevance of cross-reactive T cell populations toward gliadin epitopes in CeD is still unclear (4, 9, 18, 35, 36).

Here, we investigate specific and cross-reactive TCR recognition of disease-relevant gliadin reactive CD4$^+$ TCRs previously isolated from HLA-DQ2.5-glia-ω1$^+$ and HLA-DQ2.5-glia-α1a/ω1$^+$ tetramer sorted cells in blood and gut of HLA-DQ2.5$^+$ CeD patients (18). We show that limited CDR3β contacts with the variable residue at p7 of highly similar wheat-gliadin epitopes underpin TCR cross-reactivity. In contrast, epitope-specific recognition relied on the electrostatic environment surrounding the p7 residue. Collectively, our results provide molecular insight into TCR cross-reactivity and specificity toward gluten epitopes in HLA-DQ2.5-mediated CeD.

Results

Gliadin-reactive TCRs

We selected for study one TCR reactive to both DQ2.5-glia-ω1 and DQ2.5-glia-α1a (XPA5) and two TCRs (W316 and W321) that were DQ2.5-glia-ω1-specific, which were obtained in a previous study (18) (Table 1). The XPA5 TCR was derived from a T cell clone, TCC1383P.A.5 that had equal reactivity to DQ2.5-glia-α1a and HLA-DQ2.5-glia-ω1 (Fig. 1*A*). The W316 and W321 TCRs were derived from single cell-sorted gut T cells of two untreated CeD patients (CD1435 and CD1416) that stained with the HLA-DQ2.5-glia-ω1 tetramer but not with the HLA-DQ2.5-glia-α1a tetramer.

To further characterize the fine specificity of the XPA5 TCR, we performed a single alanine scan of both the DQ2.5-glia-α1a and HLA-DQ2.5-glia-ω1 epitopes with the TCC1383P.A.5 TCC in a proliferation assay (Fig. 1*B*). For both epitopes, the TCC lost reactivity to peptides substituted at p1-Pro, p2-Phe, p6-Glu, and p8-Pro, whereas substitutions at P7 had no effect.

Cross-reactive XPA5 TCR recognize HLA-DQ2.5-glia-α1a and HLA-DQ2.5-glia-ω1 with comparable affinity

To verify epitope-specificities of the specific and cross-reactive TCRs selected from HLA-DQ2.5-glia-α1a and HLA-DQ2.5-glia-ω1 tetramer-sorted cells in CeD patients, we performed surface plasmon resonance on recombinantly expressed proteins. For each TCR, steady-state affinities (K_D) and kinetics parameters were determined (Figs. 2 and S1 and Table 2).

The W316 TCR interacted with HLA-DQ2.5-glia-ω1 and exhibited low affinity with a K_D of ∼120 μM (Fig. 2*A*). As expected, the W321 TCR exclusively bound HLA-DQ2.5-glia-ω1 (∼25 μM) (Fig. 2*B*) (18). However, the W316 TCR weakly

Table 1
TCR gene usage of HLA-DQ2.5$^+$ T cell clones and their CDR loop sequences

TCC	Vα	Jα	CDR3α	Vβ	Dβ	Jβ	CDR3β
DQ2.5-glia-α1a/ω1-restricted TCC							
XPA5	4	43	CLVGGLARDMRF	29-1	2	2-2	CSVALGSDTGELFF
DQ2.5-glia-α1a-specific TCC							
S2[a]	4	4	CLVGDGGSFSGGYNKLIF	20-1	2	2-5	CSAGVGGQETQYF
DQ2.5-glia-ω1-specific TCCs							
W316	9-2	52	CALSGGTSYGKLTF	7-3	1	1-1	CASSQGQDTEAFF
W321	9-2	52	CALEGSAGGTSYGKLTF	7-3	2	2-3	CASSLIGGGDSTDTQYF

[a] Complexed with DQ2.5-glia-α1a epitope (LQPFPQPELPYPQ).
The TCCs 1383PA5 (abbrev. XPA5), W316, and W321 were studied in (18). The S2 TCC sequence was from (19). Nomenclature of DQ2.5 gluten epitopes follow (10). Epitope sequences were as follows: DQ2.5-glia-α1a (LQ**PFPQPELPY**; 9-mer core amino-acid sequence in bold) and DQ2.5-glia-ω1 (Q**PFPQPEQPF**P). Nomenclature of the International ImMunoGeneTics (IMGT) database used to assign TCR gene segments. Gene segments, are abbreviated as follows; Vα, TRAV; Jα, TRAJ; Vβ, TRBV; Dβ, TRBD; and Jβ, TRBJ.

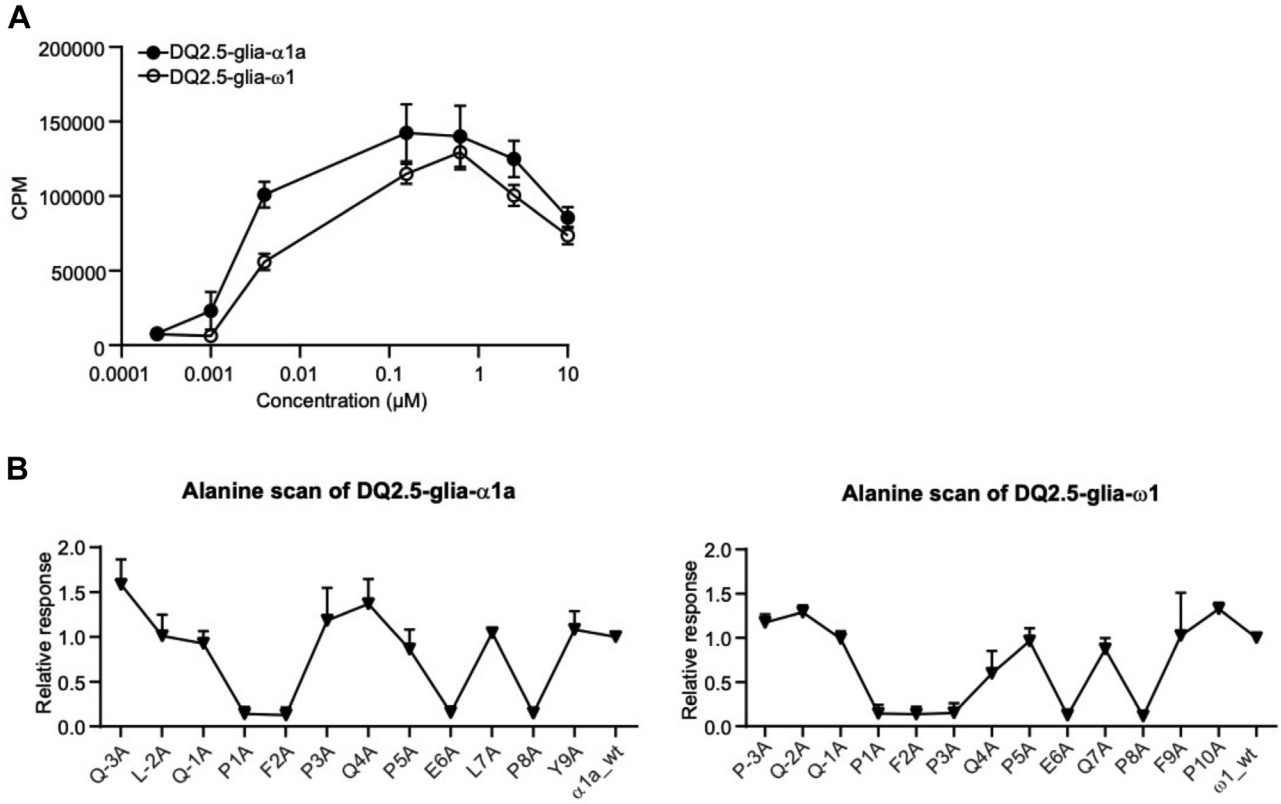

Figure 1. Cross-reactivity of TCC1383P.A.5. *A*, reactivity of TCC1383P.A.5 to titrated amounts of DQ2.5-glia-α1a and DQ2.5-glia-ω1 peptides as observed in a representative T cell proliferation assay. The y-axis shows counts per minute (CPM), whereas the x-axis shows the concentration of the peptides. The error bars represent mean ± s.d. of triplicates. Two independent experiments were performed with the same results. *B*, reactivity of TCC1383P.A.5 to the single alanine-substituted DQ2.5-glia-α1a and DQ2.5-glia-ω1 peptides tested at 10 μM in triplicates and normalized to the response to WT peptide in T cell proliferation assays. The data are derived from three independent experiments where the error bars represent mean ± s.d. TCC, T cell clone.

bound HLA-DQ2.5-glia-α1a, where the K_D was greater than 400 μM (Fig. 2*A*). Furthermore, the specific W316 and W321 TCRs displayed somewhat distinct binding kinetics with HLA-DQ2.5-glia-ω1, whereby W316 had faster on and off-rates (k_{on} = 14,900/M•s and k_{off} = 1.7/s) compared to those of W321 (k_{on} = 22,200/M•s and k_{off} = 0.5/s) (Fig. S1, *A* and *B* and Table 2).

The XPA5 TCR bound to HLA-DQ2.5-glia-α1a and HLA-DQ2.5-glia-ω1 with comparable affinity with K_D of ∼44 μM and ∼41 μM, respectively (Fig. 2*C*). These moderate affinity values of the XPA5 TCR resembled that of the cross-reactive DQ2.5-glia-α1a/ω1 L6 TCR binding to HLA-DQ2.5-glia-α1a (37 μM) we previously reported (18). Interestingly, the kinetics of the XPA5 bound to peptide-HLA (pHLA) interactions differed as XPA5-HLA-DQ2.5-glia-α1a gave slower kinetics (k_{on} = 52,700/M•s and k_{off} = 1.7/s) than the kinetics of the XPA5-HLA-DQ2.5-glia-ω1 interaction (k_{on} = 100,700/M•s and k_{off} = 3.6/s) (Fig. S1, *C* and *D* and Table 2). This indicates that the peptide variable p7 residue (p7-Leu/Gln) is affecting the on- and off-rates of the interaction (Table 2).

Structure of the W316 TCR-HLA-DQ2.5-glia-ω1 complex

To identify the molecular basis for specific recognition of DQ2.5-glia-ω1, we determined the crystal structure of the TRAV9-2$^+$-TRBV7-3$^+$ W316 TCR-HLA-DQ2.5-glia-ω1 complex to 3.0 Å resolution (Fig. 3*A* and Table S1). We previously solved the structure of the TRAV4$^+$ S2 TCR in complex with HLA-DQ2.5-glia-α1a to which it was specifically restricted (19). Similar to the S2 TCR ternary structure, the W316 TCR docked at an angle of ∼60° across the peptide-binding cleft of HLA-DQ2.5 with overall buried surface area (BSA) of ∼2030 Å^2 (Fig. 3). The W316 TCR α- and β-chains resided above HLA-DQ2.5 β- and α-chains, respectively, and thus adopted standard canonical docking polarity (Fig. 3) (37). The relative BSA contributions to the TCR-pHLA interface of the W316 TCR were CDR1β, CDR2β, and CDR3β loops were 5%, 13%, and 28%, respectively; whereas the CDR1α, CDR2α, and CDR3α loops accounted for 13%, 7%, and 20% of the BSA, respectively (Fig. 3*B*). The W316 TCR interacted with both α- and β-chains of HLA-DQ2.5. Here, the CDR1β and CDR2β loops made limited contacts with the HLA-DQ2.5 α-chain (Table S2). Thus, germline TRBV7-3 regions interacted sub-optimally with the HLA.

The germline TRAV9-2 chain of the W316 TCR mediated a salt-bridge between TCR α-framework Lys55, HLA-DQ2.5 Asp66β, and additional interactions with the HLA-DQ2.5 β-chain (Fig. 3*C* and Table S2). These interactions mediated by α-framework, CDR1α, and CDR2α loops reveal a potential basis for frequent usage of the *TRAV9-2* gene toward the HLA-DQ2.5-glia-ω1 determinant. The nongermline CDR3α loop formed a few polar-mediated interactions with the

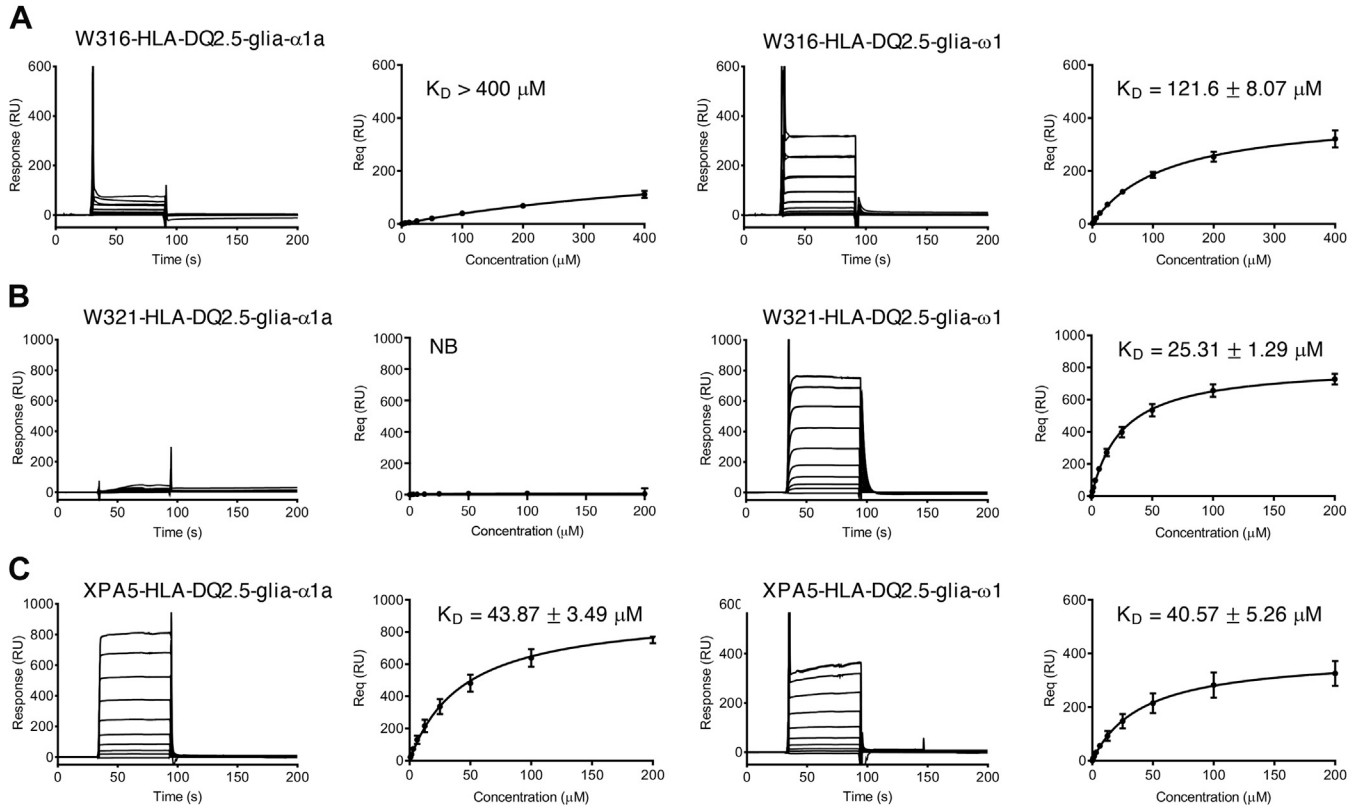

Figure 2. Surface plasmon resonance binding affinity measurements. Sensorgram and dose-response curve fit into one-site specific binding model of (*A*) W316, (*B*) W321, and (*C*) XPA5 TCR interaction with HLA-DQ2.5-glia-α1a and HLA-DQ2.5-glia-ω1. For K_D determination, all SPR data was derived from two (n = 2) independent experiments, in duplicate. Maximal concentration in dilution series of varied 200 to 400 μM. Dose-response binding curves on the *right* show mean ± s.d. from the experiments. HLA, human leukocyte antigen; KD, dissociation constant; NB, no binding; Req, Response at equilibrium; RU, response units; SPR, surface plasmon resonance; TCR, T-cell receptor.

HLA-DQ2.5 α-chain (Table S2). In contrast, the nongermline CDR3β loop of W316 TCR formed numerous interactions with the HLA-DQ2.5 β-chain, including those mediated by CDR3β Gln110 and Asp113 with HLA-DQ2.5 residues Asp66β, Ile67β, and Arg70β (Fig. 3*C* and Table S2). Notably, a hydrogen-bond between the CDR3β Asp113 β residue of the W316 TCR was formed with Arg70β of HLA-DQ2.5 located near the p7-Gln of the peptide (Fig. 3*C*). Interestingly, the position of Arg70β differs from that of the binary HLA-DQ2.5-glia-ω1 structure (18). As Arg70β in the W316 TCR-HLA-DQ2.5-glia-ω1 complex reorientated into the peptide-binding cleft and interacted with p7-Gln, thus contributing to the polar network surrounding p7-Gln (Fig. 3*C*). This polar network mediated by the CDR3β loop and Arg70β with p7-Gln would be disfavored by the hydrophobic p7-Leu of DQ2.5-glia-α1a, thereby providing a basis as to why the W316 TCR cannot recognize DQ2.5-glia-α1a. In support of this, HLA-DQ2.5-glia-α1a specific recognition by the S2 TCR did not rely on cooperative CDR3β and Arg70β interactions with p7-Leu residue (Fig. 3*D*) (18, 19).

The W316 TCR contacted p3, p5, p7, and p8 positions of the DQ2.5-glia-ω1 peptide (Fig. 3*E*). Here, the side-chains of p3-Pro, p5-Pro, and p8-Pro contacted the CDR3α loop, both CDR3 loops and the CDR2β loop, respectively. Previously, alanine-substitution of p7-Gln abolished TCR recognition of DQ2.5-glia-ω1 peptides, as direct interaction with the p7 position was lost (18). Namely, the side-chain of the p7-Gln hydrogen bonded to the backbone of the CDR3β Gln110

Table 2
Steady state binding affinities and kinetics of binding values of each TCR

HLA restriction/TCR	K_D (μM)	Bmax	k_{on} ($\times 10^3$ $M^{-1}s^{-1}$)	k_{off} (s^{-1})	K_{Dcal} (μM)	$t_{1/2}$ (s)	R^2
HLA-DQ2.5-glia-α1a							
XPA5	43.9 ± 3.5	932	52.671 ± 17.397	1.67 ± 0.40	32.6 ± 3.5	0.41	0.99
HLA-DQ2.5-glia-ω1							
XPA5	40.6 ± 5.3	393	100.745 ± 58.282	3.58 ± 1.86	36.4 ± 2.5	0.19	0.99
W316	121.6 ± 8.1	415	14.993 ± 8.162	1.67 ± 0.95	110.1 ± 4.5	0.41	0.99
W321	25.3 ± 1.3	817	22.171 ± 2.313	0.50 ± 0.03	22.5 ± 1.4	1.40	0.99

K_D, dissociation equilibrium constant of TCR-pHLA interaction. K_D is calculated using the response at the binding equilibrium (which is the data point 5 s before the end of injection). K_{Dcal}, the calculated dissociation equilibrium constant (= k_{off}/k_{on} - calculated K_D from kinetics one-site specific linear model). k_{on}, kinetic on-rate or association constant, k_{off}, kinetic off-rate or dissociation constant. $t_{1/2}$, dissociation half life. R^2, statistical goodness of fit calculated from fit to a one-site specific linear regression binding model. Similar values for K_D and K_{Dcal}, validate the kinetic parameters (k_{on} and k_{off}) are correct.

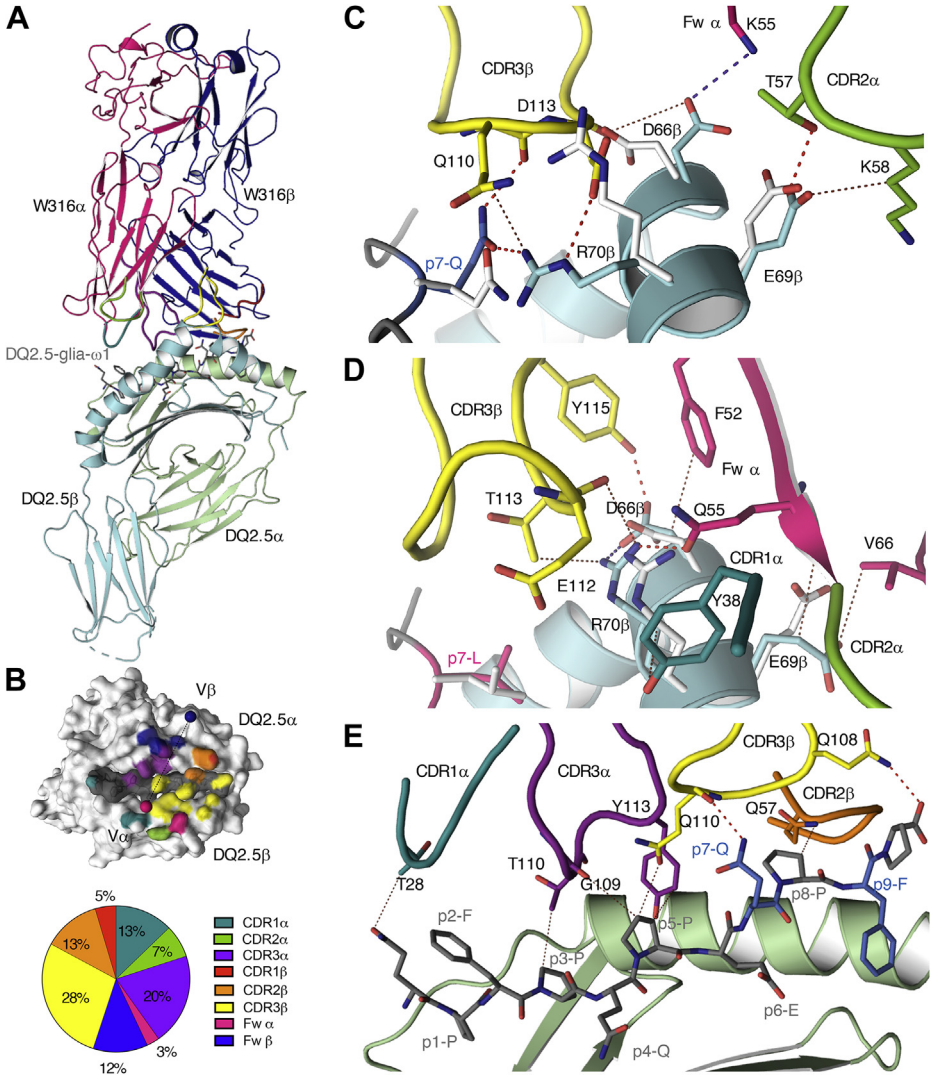

Figure 3. DQ2.5-glia-ω1-specific TCR recognition. *A*, structural overview of *TRAV9-2*$^{+}$-*TRBV7-3*$^{+}$ W316 TCR bound to HLA-DQ2.5-glia-ω1. The cartoon chains are colored as follows; HLA-DQ2.5 α-chain in *pale green*, HLA-DQ2.5 β-chain in *pale blue*, TCR α-chain in *dark pink*, and TCR β-chains in *dark blue*. The DQ2.5-glia-ω1 peptide is represented as *gray sticks*. The CDR loops are colored as follows; CDR1α, *turquoise*; CDR2α, *green*; CDR3α, *purple*; CDR1β, *red*; CDR2β, *orange*; and CDR3β, *yellow*. *B*, surface representation of TCR footprint with peptide in *gray* and TCR contact atoms are colored according to the closest CDR loop and TCR α- and β-framework contacts are colored *dark pink* and *dark blue*, respectively. The center of mass of TCR is shown by dots in *dark pink* for Vα and *dark blue* for Vβ domains connected by a *black dotted line* that indicates the approximate TCR docking angle. The pie chart shows the percentage of CDR loop and non-CDR (framework) contributions to the buried surface area (BSA). *C*, key W316 interactions between p7-glutamine of DQ2.5-glia-ω1 (*dark blue*) and surrounding HLA-DQ2.5 residues (*cyan*). Comparison of positioning of p7-adjacent HLA-DQ2.5 residues of ternary W316-HLA-DQ2.5-glia-ω1 complex with binary HLA-DQ2.5-glia-ω1 (PDB: 6MFF) complex (RMSD for HLA-DQ2.5 α-chain residues 1–79 was 0.258 Å^2) (18). *D*, key DQ2.5-glia-α1a-specific *TRAV4*$^{+}$-*TRBV20-1*$^{+}$ S2 TCR interactions between p7-leucine of DQ2.5-glia-α1a (*dark pink*) and surrounding HLA-DQ2.5 residues (*cyan*). Comparison of positioning of p7-adjacent HLA-DQ2.5 residues of ternary S2-HLA-DQ2.5-glia-α1a complex (PDB: 4OZI) with binary HLA-DQ2.5-glia-α1a (PDB: 6MFG) complex (RMSD for HLA-DQ2.5 α-chain residues 1–79 was 0.35 Å^2) (18, 19). *E*, W316 TCR interactions with DQ2.5-glia-ω1 peptide. Binary HLA-DQ2.5 residues are shown as *white stick* representation. The oxygen and nitrogen atoms are shown in *red* and *dark blue* in stick representations, respectively. *Red dashes* represent hydrogen bonds. *Purple dashes* represent salt-bridge ionic interactions. *Black dotted lines* represent van der Waals interactions. Amino acid residues are indicated by their single-letter abbreviations and lower-case p stands for position of peptide residue numbered from N-amino to C-carboxyl terminus (*left* to *right*). HLA, human leukocyte antigen; TCR, T-cell receptor.

residue. Therefore, specificity of the W316 TCR for DQ2.5-glia-ω1 was attributed to key polar contacts with p7-Gln that cannot be formed with p7-Leu of the DQ2.5-glia-α1a peptide.

Cross-reactive TCRs interact with the p7-Leu/Gln of the DQ2.5-glia-α1a and DQ2.5-glia-ω1 epitopes

To determine the structural requirements that enable cross-reactivity across the DQ2.5-glia-α1a and DQ2.5-glia-ω1 epitopes, we solved the ternary structures of the TRAV4^{+}-TRBV29-1^{+} XPA5 TCR bound to HLA-DQ2.5-glia-α1a and HLA-DQ2.5-glia-ω1 to 3.1 Å resolution (Fig. 4*A* and Table S1). The two ternary complexes were very similar to each other (r.m.sd = 0.14 Å^2), and so we shall describe the interactions within the TRAV4^{+}-TRBV29-1^{+} XPA5 TCR-HLA-DQ2.5-glia-α1a complex and highlight any salient differences to the TRAV4^{+}-TRBV29-1^{+} XPA5 TCR-HLA-DQ2.5-glia-ω1 ternary complex. The XPA5 TCR followed conventional polarity docking on HLA-DQ2.5-glia-α1a, binding at an angle of 55° (Fig. 4*B*, left) with an overall BSA

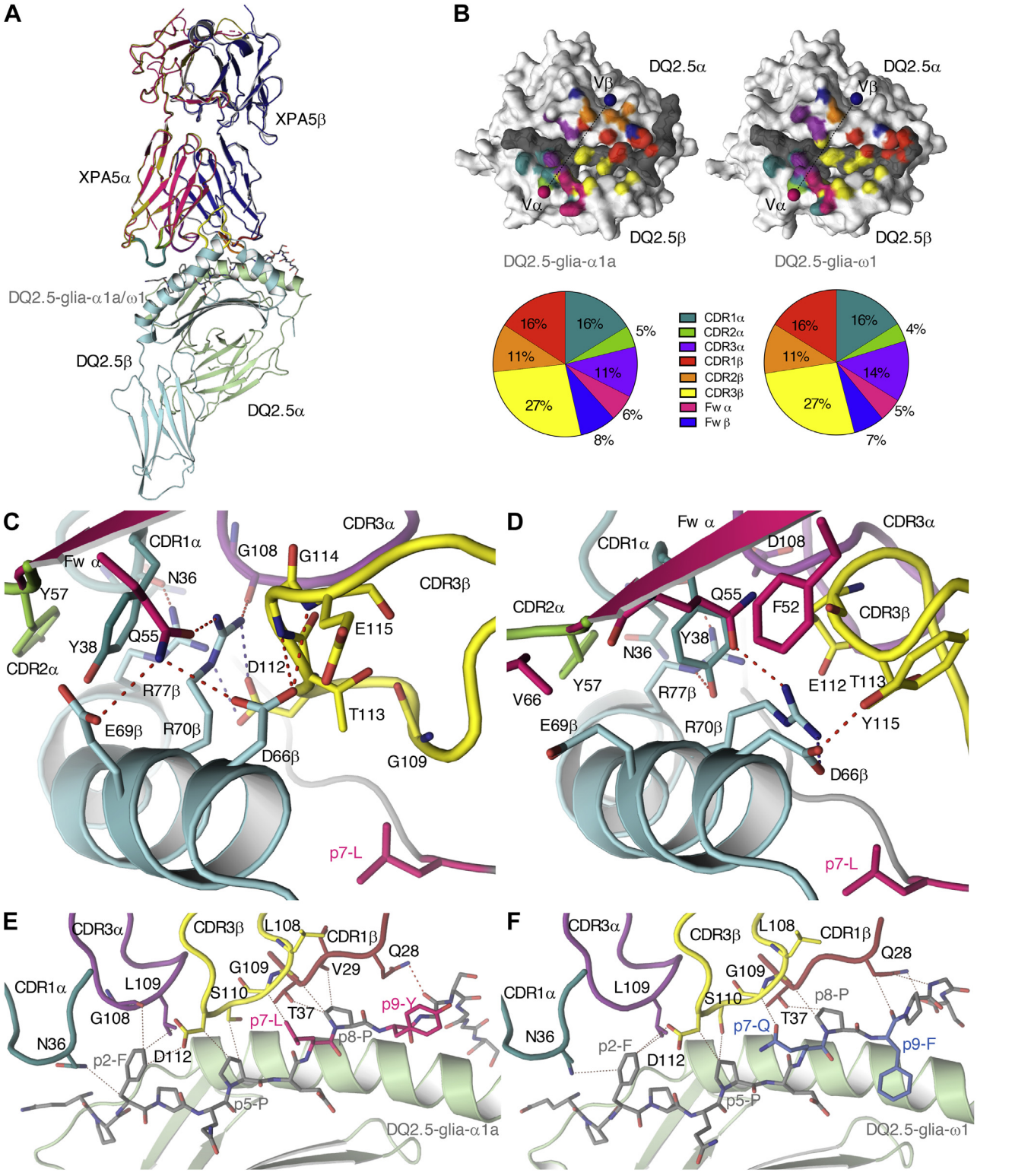

Figure 4. Cross-reactive TCR recognition of DQ2.5-glia-α1a and DQ2.5-glia-ω1 presented by HLA-DQ2.5. Structural overlay of *TRAV4*$^{+}$*-TRBV29-1*$^{+}$ XPA5 TCR-HLA-DQ2.5-glia-α1a and XPA5 TCR-HLA-DQ2.5-glia-ω1 structures (*A*). The cartoon HLA-DQ2.5 α- and β-chains are shown in *pale green* and *pale yellow*, respectively, the cartoon TCR α- and β-chains are *dark pink* and *dark blue*, respectively, with peptides represented as *gray sticks*. The CDR loops are colored as follows; CDR1α, *turquoise*; CDR2α, *green*; CDR3α, *purple*; CDR1β, *red*; CDR2β, *orange*; and CDR3β, *yellow*. Surface representation of XPA5 TCR footprint on (*B*) HLA-DQ2.5-glia-α1a (*left*) and HLA-DQ2.5-glia-ω1 (*right*), where the peptide is depicted in *gray* and TCR contact atoms are colored according to closest CDR loop, TCR α- and β-framework (FW) contacts are colored *dark pink* and *dark blue*, respectively. The center of mass of TCR is shown by dots in *dark pink* for Vα and *dark blue* for Vβ domains connected by a *black dotted line* that gives the approximate TCR docking angle. The pie chart below each footprint shows the percentage of CDR loop and non-CDR (framework) contributions to the buried surface area (BSA). Key interactions between position (p)7 of DQ2.5-glia-α1a peptide and neighboring HLA-DQ2.5-β residues with (*C*) XPA5 TCR and (*D*) S2 TCR[1]. XPA5 interactions with (*E*) DQ2.5-glia-α1a and (*F*) DQ2.5-glia-ω1 peptides. The peptides are depicted as *gray cartoon* with p7 and p9 residue that differs between DQ2.5-glia-α1a and DQ2.5-glia-ω1 peptide shown

of 2320 Å^2 at the interface (Table S3). The CDR1β, CDR1β, and CDR3β loops accounted for, 16%, 11%, and 27% of the BSA, respectively, whereas CDR1α, CDR2α, and CDR3α loops contributed to 16%, 5%, and 11% of the BSA, respectively (Fig. 4 and Table S3).

The ternary complexes of the XPA5 TCR enabled us to provide a structural basis underpinning biased usage of the TRAV4$^+$ TCR α-chain. Namely, the TRAV4 germline interactions of the XPA5 TCR were mediated by CDR1α Asn36α-Tyr38α, α-framework Gln55, and CDR2α Tyr57α with HLA-DQ2.5 β-chain as observed in the previously solved TRAV4$^+$ S2 TCR-HLA-DQ2.5-glia-α1a complex (Fig. 4, *C* and *D* and Tables S3 and S4) (19). The nongermline CDR3α loop interacted with both α- and β-chains of HLA-DQ2.5 (Fig. 4*B* and Tables S3 and S4). The germline CDR1β and CDR2β loops interacted minimally with HLA-DQ2.5, whereas the hypervariable CDR3β made extensive contacts with the HLA-DQ2.5 β-chain (Fig. 4*C* and Table S4). Here, the HLA-DQ2.5 residues Asp66β, Glu69β, and Arg70β located near the critical p7 position of both epitopes were contacted by both XPA5 TCR α- and β-chains (Fig. 4*C*). Notably, a salt-bridge between CDR3β Asp112β of XPA5 TCR was formed with Arg70β from HLA-DQ2.5, that was supplemented by polar-mediated contacts between CDR3β Thr113-Glu115, CDR3α Gly108; and germline CDR1α Asn36-Tyr38, CDR2α Gln55; and Tyr57 residues with Asp66β, Arg70β, and Arg77β of the HLA-DQ2.5 β-chain (Fig. 4*C* and Tables S3 and S4).

Regarding XPA5 TCR interactions with the DQ2.5-glia-α1a peptide, the CDR3β Asp112 residue also contacted hydrophobic side-chains of p2-Phe and p5-Pro residues (Fig. 4*E*). Moreover, the CDR1α and CDR3α loops interacted with the p2-Phe and in addition, the CDR3β loop contacted p5-Pro. The CDR1α loop contacts with p2-Phe were also observed in the TRAV4$^+$ S2 TCR specific for HLA-DQ2.5-glia-α1a, further highlighting the conserved selection of *TRAV4* encoded TCRs for this pHLA (19). The CDR1β and CDR3β loops contacted the side-chain of p8-Pro. In contrast, in the other ternary complex, the CDR1β loop contacted the backbone of p9-Phe from DQ2.5-glia-ω1 (Fig. 4*F*). Notably, the hydrophobic side chain of the DQ2.5-glia-α1a p7-Leu residue was contacted by the backbone of CDR3β Gly109 residue. The p7-Gln of DQ2.5-glia-ω1 peptide was also contacted by the backbone of CDR3β Gly109 from XPA5 TCR. Thus, the XPA5 forms conserved interactions with central peptide residues of both DQ2.5-glia-α1a and DQ2.5-glia-ω1 epitopes and readily accommodates differences at p7.

In contrast to the W316 TCR-HLA-DQ2.5-glia-ω1 complex, the p7-Gln residue of XPA5-HLA-DQ2.5-glia-ω1 complex was not contacted by Arg70β of the HLA-DQ2.5 (Table S2). Rather, in the XPA5 TCR ternary complexes, the Arg70β interacted with the TCR α- and β-chains rather than p7 of either epitope (Tables S3 and S4). Thus, the cross-reactive XPA5 TCR does not require the electrostatic pocket formed by Arg70β as observed in the W316 TCR-HLA-DQ2.5-glia-ω1 complex.

Discussion

Previously, we have described the molecular basis for antigen recognition of HLA-DQ2.5-glia-α1a and HLA-DQ2.5-glia-α2 by TCCs specifically restricted to these pHLA (19). The aforementioned HLA-DQ2.5-glia-α1a restricted S2 TCR has limited interaction with DQ2.5-glia-α1a peptide but alanine substitution of P2-Phe or P7-Gln abrogates recognition. In contrast, three ternary structures of TCRs restricted to HLA-DQ2.5-glia-α2 established the basis for the public selection of a nongermline encoded CDR3β loop Arg residue with it playing a role as a lynchpin by contacting both the DQ2.5-glia-α2 epitope and the HLA-DQ2.5 molecule (19). This arginine-linked lynchpin mechanism of antigen recognition bore a striking resemblance to what we observed for germline (CDR1α) and nongermline encoded (CDR3) Arg residues in TCRs restricted to HLA-DQ8-glia-α1 (38, 39). Hence, we established that diverse TCRs converge to form a consensus binding solution for TCR recognition of these gliadin epitopes. Further, we went on to show that T cell cross-reactivity between bacterial peptides and gliadin determinants may be a mechanism by which CeD pathogenesis is initiated. As opposed to the mechanism we have established here in this study, with respect to cross-reactivity observed for DQ2.5-glia-α1a and DQ2.5-glia-ω1, whereby differences at the key TCR contact residue p7 are tolerated, the bacterial mimic peptides required conservation of residues at key TCR contact positions (9).

In the present study, we have now provided insight into the molecular basis for epitope-specific and cross-reactive TCR recognition of two highly similar CeD-relevant epitopes, DQ2.5-glia-α1a and DQ2.5-glia-ω1.

As discussed above, this work builds on our previous study of a DQ2.5-glia-α1a specific TCR, S2, in complex with HLA-DQ2.5-glia-α1a. For specific TCR recognition of DQ2.5-glia-α1a, this TRAV4$^+$ S2 TCR did not rely on making direct p7-Leu contact, but rather contacted residues surrounding p7-Leu, such as HLA-DQ2.5 Asp66β and Arg70β (19). This is in contrast to specific TCR recognition of DQ2.5-glia-ω1 by the TRAV9-2$^+$ W316 TCR that was mediated by direct hydrogen-bonding with p7-Gln by Gln110β within the CDR3β loop. Furthermore, specific DQ2.5-glia-ω1 recognition was characterized by a shift in Arg70β from HLA-DQ2.5 to interact with p7-Gln, contributing to a polar network of interactions with and surrounding p7-Gln. This polar network would be nonpermissive for DQ2.5-glia-α1a, which possesses a hydrophobic Leu residue at the p7 position. Accordingly, specific recognition of DQ2.5-glia-α1a by the S2

as *dark pink* and *dark blue sticks*, respectively. The oxygen and nitrogen atoms are shown in *red* and *dark blue* in stick representations, respectively. *Red dashes* represent hydrogen bonds. *Purple dashes* represent salt-bridge ionic interactions. *Black dotted lines* represent van der Waals interactions. Amino acid residues are indicated by their single-letter abbreviations and lower-case p stands for position of peptide residue numbered from N-amino to C-carboxyl terminus (*left* to *right*). [1]Structure previously determined (19). HLA, human leukocyte antigen; TCR, T-cell receptor.

TCR, unlike DQ2.5-glia-ω1, did not rely on the formation of direct p7 contacts with Arg70β and CDR3β loop of TCR (19). The more flexible CDR3β loop of the S2 TCR was positioned away from the DQ2.5-glia-α1a peptide and HLA-DQ2.5 β-chain. Thus, it appears that the hypervariable CDR3β loop of W316 played a dominant role at the HLA-DQ2.5-glia-ω1 interface unlike that of S2 TCR with HLA-DQ2.5-glia-α1a. This finding provides a rationale for the fine-specificity of TCRs that were previously detected toward two immunodominant epitopes in CeD (18).

Regarding cross-reactive TCR recognition, the TRAV4$^+$ XPA5 TCR formed limited CDR3β loop contacts with p7-Leu/Gln of the DQ2.5-glia-α1a and DQ2.5-glia-ω1 epitopes. Further, unlike the reactivity assay findings on DQ2.5-glia-α1a and DQ2.5-glia-ω1 specific TCCs (18), the p7 residue (Leu/Gln) was not critical for epitope recognition by the cross-reactive T cell clone. This suggests that cross-reactivity is enabled because the TRAV4$^+$ TCR can readily accommodate P7-Gln or P7-Leu. Similar to the TRAV4$^+$ DQ2.5-glia-α1a-specific S2 TCR, the Arg70β is positioned away from p7 of peptide and interacts with the TCR α- and β-chains. Notably, XPA5 maintained the same interactions as S2 *via* the *TRAV4* germline-encoded CDR1α residues Asn36, Asp37α, and Tyr38α. However, the ternary complexes of XPA5 and S2 TCRs revealed differing modes of HLA-DQ2.5-glia-α1a recognition. Importantly, the CDR3β loop of XPA5 formed numerous interactions with central region of DQ2.5-glia-α1a peptide and HLA-DQ2.5 β-chain that were absent in the S2 ternary complex. Notably, the CDR3β loop of XPA5 associated with DQ2.5-glia-α1a in a manner analogous to the CDR3β of the TRAV8-3$^+$-TRBV5-5$^+$ LS2.8/3.15 TCR with p7-Leu of the bacterial DQ2.5-glia-α1a mimic peptide (namely, DQ2.5-*P. fluor-α1a*) as there was direct CDR3β contact with p7-Leu (9, 19). Thus, the epitope-specificity of both XPA5 and LS2.8/3.15 TCRs relies on dominant CDR3β interactions at the TCR-pHLA interface. This was also the case for the DQ2.5-*P. fluor-α1a*, DQ2.5-glia-α2/*P.aeru-α2a*, and DQ2.2-glut-L1-specific TCRs as CDR3β contacted key gluten epitope residues (19, 21). Accordingly, the hypervariable CDR3β loops of the specific and cross-reactive DQ2-restricted TCRs play a major role in mediating their interactions with pHLA complexes.

Previous studies have shed light on molecular mechanisms that may enable TCR cross-reactivity mainly in the context of autoimmune disease (31, 40). Molecular mimicry, whereby TCRs focus binding on key 'hotspot' peptide residues conserved between multiple peptide antigens while missing the differences, can account for TCR cross-reactivity (32, 40–42). In addition, dominance of the nongermline encoded CDR3 loop interactions and/or CDR3 loop flexibility has been shown to enable TCR degeneracy in recognition (9, 19, 40, 43–46). Here, the XPA5 TCR deviates from this notion as the TCR is 'ignoring' the differences between homologous gliadin epitopes. Overall, our study has provided a mechanistic understanding of TCR cross-reactivity between closely related epitopes in CeD.

Experimental procedures

T cell proliferation assay

The T cell proliferation assays were conducted, as described previously (18, 47). Briefly, 75,000 APCs (HLA-DQ2.5 homozygous Epstein-Barr virus-transformed cells) were irradiated (75 Gy) and incubated with peptides at 37 °C for 24 h. Then, 50,000 T cells were added to the cultures. Forty eight hours later, the cultures were pulsed with 1 μCi ^{3}H-thymidine. ^{3}H-thymidine incorporation was measured after 16 to 20 h later using a scintillation counter. The readout is counts per minute per well.

Protein expression and purification

The extracellular domains of HLA-DQ2.5 were expressed *via* the baculovirus-mediated insect cell expression system with gliadin epitopes covalently-linked to the N-terminus of the HLA-DQ2.5 β-chain (19, 21, 38). Sequences of gliadin epitopes in the HLA-DQ2.5 constructs are as follows: DQ2.5-glia-α1a (LQPFPQPELPY; 9-mer core amino-acid sequence underlined), DQ2.5-glia-ω1 (QPFPQPEQPFP), and DQ2.5-glia-α2 (APQPELPYPQPGS), linked to HLA-DQ2.5 β-chain *via* a flexible linker (GSGGSIEGRGGSG) (9, 18, 19). The DQ8-glia-α1 (SGEGSFQPSQENPQ) epitope was linked to the HLA-DQ8 β-chain *via* a flexible linker sequence (GGGGSIEGRGSGGG) (38). In each pHLA-DQ construct, there was a C-terminal enterokinase cleavage site (DDDK) before a leucine-zipper domain containing BirA tag for biotinylation and a polyhistidine (His) tag to assist protein purification, as previously described (9, 19). This pHLA-DQ constructs were cloned into pFastBac Dual expression vector, and the recombinant baculovirus were amplified using Sf9 insect cells (IPLB-Sf21-AE, Invitrogen). We then infected High Five (BTI-TN-5B1-4, Invitrogen) insect cells for large-scale expression of recombinant protein, as previously described (9, 19). The pHLA-DQ protein-containing supernatant was harvested after 3-days and diafiltrated into TBS-500 (0.01 M Tris pH 8.0, 0.5 M NaCl) using Cogent M1 TFF system (Merck Millipore), in line with previously established protocols (19, 20, 38). Next, His-Tag purification *via* immobilized nickel metal ion affinity chromatography (Ni-Sepharose six Fast Flow; GE Healthcare) was performed, and then protein was eluted by increasing imidazole gradient (0.02 M Imidazole pH 8.0, TBS-500–0.3 M Imidazole pH 8.0, TBS-150). After this, the protein was then purified by size exclusion chromatography (Superdex 200; GE Healthcare) and anion-exchange chromatography (HitrapQ; GE Healthcare). Before crystallization trials, the purified pHLA proteins were cleaved with enterokinase (New England Biolabs), then a final step of anion-exchange chromatography was performed.

The TCRs constructs with artificial cysteine disulfide bond in the constant regions of TCR α- and β-chains (48) were expressed in *Escherichia coli* BL21 (DE3) (19, 21, 38, 49). The αβ TCRs were purified from inclusion bodies and, subsequently, refolded as described previously (9, 38, 50). Briefly, the TCR α- and β-chains were injected in a refolding solution

containing (10 mM Tris pH 8.0, 2 mM EDTA, 5 M Urea, 0.4 M L-Arginine, 0.5 mM oxidized glutathione, and 5 mM reduced glutathione) and left stirring for 3 to 5 days at 4 °C. Subsequently, the refolding solution was dialyzed into 10 mM Tris pH 8.0 for 3 to 4 days, and then protein underwent crude anion exchange chromatography (DE52, GE Healthcare), followed by size-exclusion chromatography (Superdex 200; GE Healthcare), hydrophobic interaction chromatography (Hitrap Phenyl HP, GE Healthcare), and anion exchange chromatography (HitrapQ, GE Healthcare).

Crystallization, X-ray diffraction data collection, and processing

Sitting drop vapor diffusion crystallization experiments were performed at 20 °C. The three TCR-HLA-DQ2.5-glia-α1a/ω1 complexes were concentrated to 10 to 14 mg ml^{-1} in 0.01 M Tris at pH 8.0 and 0.15 M NaCl. Crystals that gave quality diffraction were grown from mother liquor solution, consisting of 0.25 M $(NH_4)_2SO_4$, 0.1 M Tris at pH 8.0, and 24% PEG 3350 for the W316-HLA-DQ2.5-glia-ω1 structure. The crystals of XPA5-HLA-DQ2.5-glia-α1a/ω1 structures were obtained from mother liquor composed of 0.12 to 0.14 M CaOAc, 0.01 M Tris at pH 8.0, and 16 to 18% PEG 3350. All three structures were formed in crystallization droplets with 0.5 μl of protein solution and 0.5 μl of respective mother liquor. In addition, the crystallization droplets for the XPA5-pHLA ternary complex structures were supplemented with 0.2 μl additive solution (0.01 M oxidized glutathione and 0.01 M reduced glutathione), as previously described (19). Crystals typically appeared after 3 to 7 days, were cryoprotected in 20% ethylene glycol and flash frozen in liquid nitrogen. X ray diffraction datasets were obtained at the MX2 beamline at the Australian Synchrotron (51). Data processing was performed using XDS (52) and merged using Scala of the CCP4 program suite (53, 54). The structures were solved *via* molecular replacement with Phaser (55) using search models from previously published structures of HLA-DQ2.5-glia-α1a/ω1 (PDB IDs: 6MFG, 6MFF) (18), S2 TCR (PDB: 4OZI), or using a model hybrid TCR structure constructed from the TCR α- and β-chains of BC8B and S16 TCRs (PDB IDs: 6CUG, 4OZH), respectively (19, 56). Model building, refinement, and validation were performed using Coot version 0.9 (57) Phenix program suite version 1.18.2-3874 (54, 55, 58–60). PyMOL version 2.1 (http://www.pymol.org/) was used to construct the structural figures.

Surface plasmon resonance

Surface plasmon resonance experiments were performed at 25 °C on Biacore T200 (GE Healthcare) with a Streptavidin Sensor chip (SA) (GE Healthcare). HBS-EP buffer (10 mM Hepes pH 7.5, 150 mM NaCl, 2 mM EDTA, and 0.005% Tween 20) was used as a running buffer in all subsequent binding experiment with a flow rate of 30 μl/min. Biotinylated HLA-DQ2.5-glia-α1a, HLA-DQ2.5-glia-ω1, mouse MHC-I molecule $H2D^b$-$Na_{181\text{-}191}$ (background control), and HLA-DQ2.5-glia-α2/DQ8-glia-α1 (negative controls) were coupled to SA chip using HBS buffer (10 mM HEPES pH 7.5, 150 mM NaCl) at a flow rate of 5 μl/min. Subsequently, an injection of 1 mM of biotin was performed to block the remaining free streptavidin binding sites. On average 3000 Response Units of protein were immobilized.

The XPA5, W316, and W321 TCRs were injected over the surface in a series of eight concentrations with a maximum of 200 to 400 μM (contact time: 60 s; dissociation time: 200s)

Experiments were performed in duplicates, and the equilibrium dissociation constant, K_D, was determined from either two or three independent experiments using GraphPad Prism version 8.0.

Data availability

The structures were deposited in the PDB database (PDB codes for ternary complexes; W316-HLA-DQ2.5-glia-ω1, 7SG0; XPA5-HLA-DQ2.5-glia-α1a, 7SG1S3SS; and XPA5-HLA-DQ2.5-glia-ω1, 7SG2).

Supporting information—This article contains supporting information.

Acknowledgments—We thank the Monash Molecular Crystallization Facility for his assistance with crystallization. The protein crystal X-ray diffraction data were collected on MX2 beamline at the Australian Synchrotron facility, Melbourne, Australia.

Author contributions—L. C. and S. D.-K. investigation; L. C., C. F., S. D.-K., J. P., and H. H. R. formal analysis; L. C. and J. R. writing–original draft; C. F., J. P., and H. H. R. supervision; C. F., S. D.-K., J. P., L. M. S., and J. R. writing–review and editing; S. D.-K. and L. M. S. resources; S. D.-K., L. M. S., and J. R. methodology.

Funding and additional information—This work was supported by the National Health and Medical Research Council of Australia and by the South-Eastern Norway Regional Health Authority (projects 2011050 and 2015009), the Research Council of Norway (project 179573/V40 through the Centre of Excellence funding scheme and project 233885) and by Stiftelsen Kristian Gerhard Jebsen (project SKGJ-MED-017) to L. M. S.; J. R. is supported by an ARC Australian Laureate Fellowship.

Conflict of interest—The authors declare that they have no conflict of interest with the contents of this article.

Abbreviations—The abbreviations used are: BSA, buried surface area; CeD, Celiac disease; HLA, human leukocyte antigen; p7, position 7; pHLA, peptide HLA; TCCs, T cell clones; TCR, T-cell receptor; TG2, transglutaminase 2; TRAV, T-cell receptor alpha variable; TRBV, T-cell receptor beta variable.

References

1. Singh, P., Arora, A., Strand, T. A., Leffler, D. A., Catassi, C., Green, P. H., Kelly, C. P., Ahuja, V., and Makharia, G. K. (2018) Global prevalence of celiac disease: Systematic review and meta-analysis. *Clin. Gastroenterol. Hepatol.* **16**, 823–836.e2
2. Sollid, L. M. (2002) Coeliac disease: Dissecting a complex inflammatory disorder. *Nat. Rev. Immunol.* **2**, 647–655

3. Falcigno, L., Calvanese, L., Conte, M., Nanayakkara, M., Barone, M. V., and D'Auria, G. (2020) Structural perspective of gliadin peptides active in celiac disease. *Int. J. Mol. Sci.* **21**, 9301
4. Hardy, M. Y., Russell, A. K., Pizzey, C., Jones, C. M., Watson, K. A., La Gruta, N. L., Cameron, D. J., and Tye-Din, J. A. (2020) Characterisation of clinical and immune reactivity to barley and rye ingestion in children with coeliac disease. *Gut* **69**, 830–840
5. Jabri, B., and Sollid, L. M. (2009) Tissue-mediated control of immunopathology in coeliac disease. *Nat. Rev. Immunol.* **9**, 858–870
6. Kagnoff, M. F. (2007) Celiac disease: Pathogenesis of a model immunogenetic disease. *J. Clin. Invest.* **117**, 41–49
7. Koning, F. (2005) Celiac disease: Caught between a rock and a hard place. *Gastroenterology* **129**, 1294–1301
8. Lindeman, I., Zhou, C., Eggesbø, L. M., Miao, Z., Polak, J., Lundin, K. E., Jahnsen, J., Qiao, S.-W., Iversen, R., and Sollid, L. M. (2020) Longevity, clonal relationship, and transcriptional program of celiac disease–specific plasma cells. *J. Exp. Med.* **218**, e20200852
9. Petersen, J., Ciacchi, L., Tran, M. T., Loh, K. L., Kooy-Winkelaar, Y., Croft, N. P., Hardy, M. Y., Chen, Z., McCluskey, J., and Anderson, R. P. (2020) T cell receptor cross-reactivity between gliadin and bacterial peptides in celiac disease. *Nat. Struct. Mol. Biol.* **27**, 49–61
10. Sollid, L. M., Tye-Din, J. A., Qiao, S.-W., Anderson, R. P., Gianfrani, C., and Koning, F. (2020) Update 2020: Nomenclature and listing of celiac disease–relevant gluten epitopes recognized by CD4+ T cells. *Immunogenetics* **72**, 85–88
11. Tye-Din, J. A., Stewart, J. A., Dromey, J. A., Beissbarth, T., van Heel, D. A., Tatham, A., Henderson, K., Mannering, S. I., Gianfrani, C., and Jewell, D. P. (2010) Comprehensive, quantitative mapping of T cell epitopes in gluten in celiac disease. *Sci. Transl. Med.* **2**, 41ra51
12. Yao, Y., Zia, A., Neumann, R. S., Pavlovic, M., Balaban, G., Lundin, K. E., Sandve, G. K., and Qiao, S. W. (2021) T cell receptor repertoire as a potential diagnostic marker for celiac disease. *Clin. Immunol.* **222**, 108621
13. Fleckenstein, B., Molberg, O., Qiao, S. W., Schmid, D. G., von der Mulbe, F., Elgstoen, K., Jung, G., and Sollid, L. M. (2002) Gliadin T cell epitope selection by tissue transglutaminase in celiac disease. Role of enzyme specificity and pH influence on the transamidation *versus* deamidation process. *J. Biol. Chem.* **277**, 34109–34116
14. Molberg, O., McAdam, S. N., Korner, R., Quarsten, H., Kristiansen, C., Madsen, L., Fugger, L., Scott, H., Noren, O., Roepstorff, P., Lundin, K. E., Sjostrom, H., and Sollid, L. M. (1998) Tissue transglutaminase selectively modifies gliadin peptides that are recognized by gut-derived T cells in celiac disease. *Nat. Med.* **4**, 713–717
15. Vader, L. W., Stepniak, D. T., Bunnik, E. M., Kooy, Y. M., De Haan, W., Drijfhout, J. W., Van Veelen, P. A., and Koning, F. (2003) Characterization of cereal toxicity for celiac disease patients based on protein homology in grains. *Gastroenterology* **125**, 1105–1113
16. van de Wal, Y., Kooy, Y., van Veelen, P., Pena, S., Mearin, L., Papadopoulos, G., and Koning, F. (1998) Selective deamidation by tissue transglutaminase strongly enhances gliadin-specific T cell reactivity. *J. Immunol.* **161**, 1585–1588
17. Kim, C.-Y., Quarsten, H., Bergseng, E., Khosla, C., and Sollid, L. M. (2004) Structural basis for HLA-DQ2-mediated presentation of gluten epitopes in celiac disease. *Proc. Natl. Acad. Sci. U. S. A.* **101**, 4175–4179
18. Dahal-Koirala, S., Ciacchi, L., Petersen, J., Risnes, L. F., Neumann, R. S., Christophersen, A., Lundin, K. E., Reid, H. H., Qiao, S.-W., and Rossjohn, J. (2019) Discriminative T-cell receptor recognition of highly homologous HLA-DQ2–bound gluten epitopes. *J. Biol. Chem.* **294**, 941–952
19. Petersen, J., Montserrat, V., Mujico, J. R., Loh, K. L., Beringer, D. X., Van Lummel, M., Thompson, A., Mearin, M. L., Schweizer, J., and Kooy-Winkelaar, Y. (2014) T-cell receptor recognition of HLA-DQ2–gliadin complexes associated with celiac disease. *Nat. Struct. Mol. Biol.* **21**, 480–488
20. Henderson, K. N., Tye-Din, J. A., Reid, H. H., Chen, Z., Borg, N. A., Beissbarth, T., Tatham, A., Mannering, S. I., Purcell, A. W., and Dudek, N. L. (2007) A structural and immunological basis for the role of human leukocyte antigen DQ8 in celiac disease. *Immunity* **27**, 23–34
21. Ting, Y. T., Dahal-Koirala, S., Kim, H. S. K., Qiao, S.-W., Neumann, R. S., Lundin, K. E., Petersen, J., Reid, H. H., Sollid, L. M., and Rossjohn, J. (2020) A molecular basis for the T cell response in HLA-DQ2.2 mediated celiac disease. *Proc. Natl. Acad. Sci. U. S. A.* **117**, 3063–3073
22. Høydahl, L. S., Richter, L., Frick, R., Snir, O., Gunnarsen, K. S., Landsverk, O. J., Iversen, R., Jeliazkov, J. R., Gray, J. J., Bergseng, E., and Foss, S. (2019) Plasma cells are the most abundant gluten peptide MHC-expressing cells in inflamed intestinal tissues from patients with celiac disease. *Gastroenterology* **156**, 1428–1439
23. Di Niro, R., Mesin, L., Zheng, N.-Y., Stamnaes, J., Morrissey, M., Lee, J.-H., Huang, M., Iversen, R., Du Pré, M. F., and Qiao, S.-W. (2012) High abundance of plasma cells secreting transglutaminase 2–specific IgA autoantibodies with limited somatic hypermutation in celiac disease intestinal lesions. *Nat. Med.* **18**, 441–445
24. Dahal-Koirala S, N. R., Jahnsen, J., Lundin, K. E. A., and Sollid, L. M. (2020) On the immune response to barley in celiac disease: Biased and public T-cell receptor usage to a barley unique and immunodominant gluten epitope. *Eur. J. Immunol.* **50**, 256–269
25. Christophersen, A., Risnes, L. F., Bergseng, E., Lundin, K. E., Sollid, L. M., and Qiao, S. W. (2016) Healthy HLA-DQ2.5+ subjects lack regulatory and memory T cells specific for immunodominant gluten epitopes of celiac disease. *J. Immunol.* **196**, 2819–2826
26. Qiao, S.-W., Christophersen, A., Lundin, K. E., and Sollid, L. M. (2014) Biased usage and preferred pairing of α-and β-chains of TCRs specific for an immunodominant gluten epitope in coeliac disease. *Int. Immunol.* **26**, 13–19
27. Dahal-Koirala, S., Risnes, L., Christophersen, A., Sarna, V., Lundin, K. E., Sollid, L., and Qiao, S. (2016) TCR sequencing of single cells reactive to DQ2.5-glia-α2 and DQ2.5-glia-ω2 reveals clonal expansion and epitope-specific V-gene usage. *Mucosal Immunol.* **9**, 587–596
28. Arentz-Hansen, H., Körner, R., Molberg, Ø., Quarsten, H., Vader, W., Kooy, Y. M., Lundin, K. E., Koning, F., Roepstorff, P., and Sollid, L. M. (2000) The intestinal T cell response to α-gliadin in adult celiac disease is focused on a single deamidated glutamine targeted by tissue transglutaminase. *J. Exp. Med.* **191**, 603–612
29. Vader, W., Stepniak, D., Kooy, Y., Mearin, L., Thompson, A., van Rood, J. J., Spaenij, L., and Koning, F. (2003) The HLA-DQ2 gene dose effect in celiac disease is directly related to the magnitude and breadth of gluten-specific T cell responses. *Proc. Natl. Acad. Sci. U. S. A.* **100**, 12390–12395
30. Qiao, S.-W., Dahal-Koirala, S., Eggesbø, L. M., Lundin, K. E., and Sollid, L. M. (2021) Frequency of gluten-reactive T cells in active celiac lesions estimated by direct cell cloning. *Front. Immunol.* **12**, 646163
31. Sethi, D. K., Schubert, D. A., Anders, A.-K., Heroux, A., Bonsor, D. A., Thomas, C. P., Sundberg, E. J., Pyrdol, J., and Wucherpfennig, K. W. (2011) A highly tilted binding mode by a self-reactive T cell receptor results in altered engagement of peptide and MHC. *J. Exp. Med.* **208**, 91–102
32. Harkiolaki, M., Holmes, S. L., Svendsen, P., Gregersen, J. W., Jensen, L. T., McMahon, R., Friese, M. A., Van Boxel, G., Etzensperger, R., and Tzartos, J. S. (2009) T cell-mediated autoimmune disease due to low-affinity crossreactivity to common microbial peptides. *Immunity* **30**, 348–357
33. Cole, D. K., Bulek, A. M., Dolton, G., Schauenberg, A. J., Szomolay, B., Rittase, W., Trimby, A., Jothikumar, P., Fuller, A., and Skowera, A. (2016) Hotspot autoimmune T cell receptor binding underlies pathogen and insulin peptide cross-reactivity. *J. Clin. Invest.* **126**, 2191–2204
34. Hardy, M. Y., Tye-Din, J. A., Stewart, J. A., Schmitz, F., Dudek, N. L., Hanchapola, I., Purcell, A. W., and Anderson, R. P. (2015) Ingestion of oats and barley in patients with celiac disease mobilizes cross-reactive T cells activated by avenin peptides and immuno-dominant hordein peptides. *J. Autoimmun.* **56**, 56–65
35. Gunnarsen, K. S., Høydahl, L. S., Risnes, L. F., Dahal-Koirala, S., Neumann, R. S., Bergseng, E., Frigstad, T., Frick, R., du Pré, M. F., Dalhus, B., and Lundin, K. E. (2017) A TCRα framework–centered codon shapes a biased T cell repertoire through direct MHC and CDR3β interactions. *JCI Insight* **2**, e95193
36. Hardy, M. Y., Girardin, A., Pizzey, C., Cameron, D. J., Watson, K. A., Picascia, S., Auricchio, R., Greco, L., Gianfrani, C., and La Gruta, N. L.

(2015) Consistency in polyclonal T-cell responses to gluten between children and adults with celiac disease. *Gastroenterology* **149**, 1541–1552
37. La Gruta, N. L., Gras, S., Daley, S. R., Thomas, P. G., and Rossjohn, J. (2018) Understanding the drivers of MHC restriction of T cell receptors. *Nat. Rev. Immunol.* **18**, 467–478
38. Broughton, S. E., Petersen, J., Theodossis, A., Scally, S. W., Loh, K. L., Thompson, A., van Bergen, J., Kooy-Winkelaar, Y., Henderson, K. N., and Beddoe, T. (2012) Biased T cell receptor usage directed against human leukocyte antigen DQ8-restricted gliadin peptides is associated with celiac disease. *Immunity* **37**, 611–621
39. Petersen, J., Kooy-Winkelaar, Y., Loh, K. L., Tran, M., Van Bergen, J., Koning, F., Rossjohn, J., and Reid, H. H. (2016) Diverse T cell receptor gene usage in HLA-DQ8-associated celiac disease converges into a consensus binding solution. *Structure* **24**, 1643–1657
40. Sethi, D. K., Gordo, S., Schubert, D. A., and Wucherpfennig, K. W. (2013) Crossreactivity of a human autoimmune TCR is dominated by a single TCR loop. *Nat. Commun.* **4**, 2623
41. Lang, H. L., Jacobsen, H., Ikemizu, S., Andersson, C., Harlos, K., Madsen, L., Hjorth, P., Sondergaard, L., Svejgaard, A., and Wucherpfennig, K. (2002) A functional and structural basis for TCR cross-reactivity in multiple sclerosis. *Nat. Immunol.* **3**, 940–943
42. Hahn, M., Nicholson, M. J., Pyrdol, J., and Wucherpfennig, K. W. (2005) Unconventional topology of self peptide–major histocompatibility complex binding by a human autoimmune T cell receptor. *Nat. Immunol.* **6**, 490–496
43. Reiser, J.-B., Darnault, C., Grégoire, C., Mosser, T., Mazza, G., Kearney, A., van der Merwe, P. A., Fontecilla-Camps, J. C., Housset, D., and Malissen, B. (2003) CDR3 loop flexibility contributes to the degeneracy of TCR recognition. *Nat. Immunol.* **4**, 241–247
44. Scott, D. R., Borbulevych, O. Y., Piepenbrink, K. H., Corcelli, S. A., and Baker, B. M. (2011) Disparate degrees of hypervariable loop flexibility control T-cell receptor cross-reactivity, specificity, and binding mechanism. *J. Mol. Biol.* **414**, 385–400
45. Borbulevych, O. Y., Piepenbrink, K. H., Gloor, B. E., Scott, D. R., Sommese, R. F., Cole, D. K., Sewell, A. K., and Baker, B. M. (2009) T cell receptor cross-reactivity directed by antigen-dependent tuning of peptide-MHC molecular flexibility. *Immunity* **31**, 885–896
46. Borg, N. A., Ely, L. K., Beddoe, T., Macdonald, W. A., Reid, H. H., Clements, C. S., Purcell, A. W., Kjer-Nielsen, L., Miles, J. J., and Burrows, S. R. (2005) The CDR3 regions of an immunodominant T cell receptor dictate the'energetic landscape'of peptide-MHC recognition. *Nat. Immunol.* **6**, 171–180
47. Christophersen, A., Ráki, M., Bergseng, E., Lundin, K. E., Jahnsen, J., Sollid, L. M., and Qiao, S. W. (2014) Tetramer-visualized gluten-specific CD4+ T cells in blood as a potential diagnostic marker for coeliac disease without oral gluten challenge. *United European Gastroenterol. J.* **2**, 268–278
48. Boulter, J. M., Glick, M., Todorov, P. T., Baston, E., Sami, M., Rizkallah, P., and Jakobsen, B. K. (2003) Stable, soluble T-cell receptor molecules for crystallization and therapeutics. *Protein Eng.* **16**, 707–711
49. Clements, C. S., Kjer-Nielsen, L., MacDonald, W. A., Brooks, A. G., Purcell, A. W., McCluskey, J., and Rossjohn, J. (2002) The production, purification and crystallization of a soluble heterodimeric form of a highly selected T-cell receptor in its unliganded and liganded state. *Acta Crystallogr. D Biol. Crystallogr.* **58**, 2131–2134
50. Petersen, J., van Bergen, J., Loh, K. L., Kooy-Winkelaar, Y., Beringer, D. X., Thompson, A., Bakker, S. F., Mulder, C. J., Ladell, K., and McLaren, J. E. (2015) Determinants of gliadin-specific T cell selection in celiac disease. *J. Immunol.* **194**, 6112–6122
51. Aragão, D., Aishima, J., Cherukuvada, H., Clarken, R., Clift, M., Cowieson, N. P., Ericsson, D. J., Gee, C. L., Macedo, S., and Mudie, N. (2018) MX2: A high-flux undulator microfocus beamline serving both the chemical and macromolecular crystallography communities at the Australian Synchrotron. *J. Synchrotron Radiat.* **25**, 885–891
52. Kabsch, W. (2010) XDS. *Acta Crystallogr. D Biol. Crystallogr.* **66**, 125–132
53. Winn, M. D., Ballard, C. C., Cowtan, K. D., Dodson, E. J., Emsley, P., Evans, P. R., Keegan, R. M., Krissinel, E. B., Leslie, A. G., and McCoy, A. (2011) Overview of the CCP4 suite and current developments. *Acta Crystallogr. D Biol. Crystallogr.* **67**, 235–242
54. Liebschner, D., Afonine, P. V., Baker, M. L., Bunkóczi, G., Chen, V. B., Croll, T. I., Hintze, B., Hung, L.-W., Jain, S., and McCoy, A. J. (2019) Macromolecular structure determination using X-rays, neutrons and electrons: Recent developments in Phenix. *Acta Crystallogr. D Struct. Biol.* **75**, 861–877
55. McCoy, A. J. (2007) Solving structures of protein complexes by molecular replacement with Phaser. *Acta Crystallogr. D Biol. Crystallogr.* **63**, 32–41
56. Shahine, A., Reinink, P., Reijneveld, J. F., Gras, S., Holzheimer, M., Cheng, T.-Y., Minnaard, A. J., Altman, J. D., Lenz, S., Prandi, J., Kubler-Kielb, J., Moody, D. B., Rossjohn, J., and Van Rhijn, I. (2019) A T-cell receptor escape channel allows broad T-cell response to CD1b and membrane phospholipids. *Nat. Commun.* **10**, 56
57. Emsley, P., Lohkamp, B., Scott, W. G., and Cowtan, K. (2010) Features and development of Coot. *Acta Crystallogr. D Biol. Crystallogr.* **66**, 486–501
58. Williams, C. J., Headd, J. J., Moriarty, N. W., Prisant, M. G., Videau, L. L., Deis, L. N., Verma, V., Keedy, D. A., Hintze, B. J., and Chen, V. B. (2018) MolProbity: More and better reference data for improved all-atom structure validation. *Protein Sci.* **27**, 293–315
59. Afonine, P. V., Grosse-Kunstleve, R. W., Echols, N., Headd, J. J., Moriarty, N. W., Mustyakimov, M., Terwilliger, T. C., Urzhumtsev, A., Zwart, P. H., and Adams, P. D. (2012) Towards automated crystallographic structure refinement with phenix.refine. *Acta Crystallogr. D Biol. Crystallogr.* **68**, 352–367
60. Adams, P. D., Afonine, P. V., Bunkóczi, G., Chen, V. B., Davis, I. W., Echols, N., Headd, J. J., Hung, L.-W., Kapral, G. J., and Grosse-Kunstleve, R. W. (2010) Phenix: A comprehensive Python-based system for macromolecular structure solution. *Acta Crystallogr. D Biol. Crystallogr.* **66**, 213–221